



# Properties of Relativistic, Compact Stars

Alexander W. Ho

February 2007

Publication Number: CSRCR2007-07

Computational Science &  
Engineering Faculty and Students  
Research Articles

Database Powered by the  
Computational Science Research Center  
Computing Group

## COMPUTATIONAL SCIENCE & ENGINEERING



**SAN DIEGO STATE  
UNIVERSITY**

Computational Science Research Center  
College of Sciences  
5500 Campanile Drive  
San Diego, CA 92182-1245  
(619) 594-3430



# PROPERTIES OF RELATIVISTIC, COMPACT STARS

---

A Thesis

Presented to the

Faculty of

San Diego State University

---

In Partial Fulfillment

of the Requirements for the Degree

Master of Science

in

Physics

---

by

Alexander W Ho

Spring 2006

**SAN DIEGO STATE UNIVERSITY**

The Undersigned Faculty Committee Approves the

Thesis of Alexander W Ho:

Properties of Relativistic, Compact Stars

---

Fridolin Weber, Chair  
Department of Physics

---

Calvin Johnson  
Department of Physics

---

Jerome Orosz  
Department of Astronomy

---

Approval Date

Copyright © 2006

by

Alexander W Ho

All Rights Reserved

## **ABSTRACT OF THE THESIS**

Properties of Relativistic, Compact Stars

by

Alexander W Ho

Master of Science in Physics

San Diego State University, 2006

Compact stars are extremely dense objects with very interesting properties. Not only are they of great interest to astrophysicists, but their dense nature provides an excellent testing area for a variety of phenomena and exotic particles that may prove significant to many different areas of physics as well. One particular subject is that of strangeness and strange quark stars. This paper investigates such stars as well as their nuclear counterparts, neutron stars. The properties of relativistic neutron stars are examined as well as the impact of strangeness on compact astronomical objects.

## TABLE OF CONTENTS

	PAGE
ABSTRACT .....	iv
LIST OF TABLES .....	vi
LIST OF FIGURES .....	vii
ACKNOWLEDGEMENTS .....	ix
CHAPTER	
1 INTRODUCTION .....	1
2 RELATIVISTIC STARS/COMPACT STARS IN GENERAL RELATIVITY .....	3
Einstein's Equations .....	3
Spherical Stars .....	4
Rotating Stars .....	5
3 EQUATIONS OF STATE .....	8
Conventional Neutron-Star Matter .....	8
Strange Matter .....	12
4 RESULTS .....	15
Neutron Stars .....	16
Quark Stars .....	29
5 SUMMARY .....	37
REFERENCES .....	41
APPENDIX	
SAMPLE EOS .....	44

## LIST OF TABLES

	PAGE
Table 1. Summary of Neutron Star Matter Equations of State. Additional Properties Displayed in Tables 2 and 3.....	10
Table 2. Properties of Equations of State listed in Table 1.....	11
Table 3. Properties of Nuclear Matter at Saturation Density of Equations of State from Table 1. The Quantities in this Table are: Energy per Baryon $E/A$ , Incompressibility $K$ , Effective Nucleon Mass $M^*$ ( $\equiv m^*_N/m_N$ ), and Symmetry Energy $a_{\text{sym}}$ .....	11
Table 4. Candidates for Heavy Neutron Stars .....	17

## LIST OF FIGURES

	PAGE
Figure 1. Comparison of mass (in solar masses) versus radius (km) for this series of compact stars. This figure compares these properties for both rotating and spherically symmetric versions of these stars.....	17
Figure 2. Comparison of pressure versus energy-density for compact star equations of state. The uppermost line represents the limit EOS, where pressure equals energy-density. Any EOS past it would violate causality.....	19
Figure 3. Mass versus energy-density for sequence of non-rotating neutron stars.....	20
Figure 4. Mass versus energy-density for sequence of rotating neutron stars.....	20
Figure 5. Mass versus the range of possible densities for the sequence of non-rotating neutron stars.....	21
Figure 6. Mass versus the range of possible densities for the sequence of rotating neutron stars.....	21
Figure 7. Comparison of mass versus range of possible densities for this sequence of rotating and non-rotating stars.....	22
Figure 8. Moment of Inertia for compact stars versus their mass (in solar masses). The classical moment of inertia for EOS <i>ehv</i> has also been shown for comparison. Note the substantial change when relativistic effects are taken into account.....	23
Figure 9. Mass (in solar masses) versus surface gravity in units of $10^{14}$ cm/s <sup>2</sup> for star masses near 1.3 solar masses.....	24
Figure 10. Mass (in solar masses) versus surface gravity in units of $10^{14}$ cm/s <sup>2</sup> for exact masses of 1.3, 1.35, and 1.4 $M_{\text{sol}}$ . Ewal-cfl-mixed points for 1.35 and 1.4 $M_{\text{sol}}$ have values greater than allowed on this plot.....	25
Figure 11. Shown here are the limiting masses and corresponding surface gravities (in units of $10^{14}$ g/cm <sup>2</sup> ) for this sequence of compact stars.....	26
Figure 12. Surface gravity versus mass for neutron stars. Full spectrum is shown.....	26
Figure 13. Kepler (mass shedding) frequency of compact stars versus their masses (in units of solar mass). Frequencies of observed stars have been shaded. Observed stars rotate below the mass shedding frequency.....	28
Figure 14. Kepler (mass shedding) period versus mass (in solar masses) for sequence of stars. Observed stars rotate above the mass shedding period.....	29



Figure 15. Comparison of mass versus radius for a strange quark star with bag constant $B^{1/4} = 145$ MeV. The crust energy-density has been set for two different values.....	30
Figure 16. Comparison of mass versus radius for a strange quark star with bag constant $B^{1/4} = 160$ MeV. The crust energy-density has been set for two different values.....	31
Figure 17. Mass (in solar masses) versus radius for strange quark stars. Shown are a comparison of rotating and non-rotating sequences for different bag constants .....	32
Figure 18. Surface gravity as a function of mass (in solar masses) for strange quark stars with different bag constants.....	33
Figure 19. Baryon number of crust versus baryon number of core for bag constants $B^{1/4} = 145$ MeV, 160 MeV.....	34
Figure 20. Baryon number of crust versus radius of strange quark matter core for bag constants $B^{1/4} = 145$ MeV, 160 MeV .....	35
Figure 21. Crust mass versus total mass of strange quark star for bag constants $B^{1/4} = 145$ MeV, 160 MeV .....	36
Figure 22. Crust mass versus total radius of strange quark star for bag constants $B^{1/4} = 145$ MeV, 160 MeV .....	36
Figure 24. Comparison of equations of state for the Indian model to the MIT bag model, $B^{1/4} = 145$ MeV and 160 MeV .....	39

## **ACKNOWLEDGEMENTS**

The author of this thesis would like to thank Dr. Fridolin Weber for his encouragement and help, as well as the countless hours of discussion and assistance that has made this work possible. Dr. Weber's ideas and suggestions have proven invaluable in the progress of this thesis. The author would also like to sincerely thank Dr. Calvin Johnson and Dr. Jerome Orosz for serving on his thesis committee.

## CHAPTER 1

### INTRODUCTION

Stellar objects have fascinated people since the beginning of mankind. Consequently, research has been conducted for centuries trying to discover the true nature of these items. As technology has grown, so has man's understanding of the cosmos, bringing us to the present time where we are optically able to resolve images from across the universe and can put objects into orbit about planets throughout our solar system. An area of particular interest is stars; their composition, properties, interactions, etc. One specific class of stars, namely, compact stars (white dwarfs, "neutron stars", and black holes), is of great interest and importance to astrophysicists, as well as nuclear and particle physicists alike.

Neutron stars are extremely dense and massive objects with very interesting properties. They also host a variety of fascinating properties due to their dense nature. These stars are neutron-rich, and typically only have a radius of  $\sim 10$  km, though their mass is approximately the same as our sun ( $M_{\text{sol}} \approx 2 \times 10^{30}$  kg). Since these stars are so dense, up to 10-20 times the density of atomic nuclei ( $\rho_0 = 2.5 \times 10^{14}$  g/cm<sup>3</sup>), the core is given the opportunity to be host to a variety of exotic particles/phases (such as hyperons, quarks, and bosons), and processes [1,2,3]. One class of these particles that has gained an increased interest is strange quarks and strange quark matter. Strange quark matter may be more stable than atomic nuclei, and could even explain the problem of "missing matter" (dark matter). If it were more stable than atomic nuclei, this would imply that all neutron stars have a potential for possessing a strange quark core, covered in a nuclear crust layer [4]. Even more remarkable is the fact that neutrons within such a crust exceeding the neutron drip density

would detach from the crust into a superconducting gap and be transformed into strange quark matter themselves. Although this idea of strange stars [5,6,7] is not new, it is of great interest to astrophysicists and physicists in general since these stars could offer insight into a wide range of exciting astrophysical phenomena. In this paper I will investigate properties of standard “neutron” stars, as well as those of strange quark stars.

## CHAPTER 2

### COMPACT STARS IN GENERAL RELATIVITY

Due to the fact that neutron stars are extremely dense (typically 10-20 times  $\rho_0$ ), calculations must be treated within the framework of Einstein's theory of general relativity. However, there are many components that must be considered when applying relativistic concepts. It is imperative that relativity be considered since many aspects of these stars are directly affected and altered due to Einstein's equations, showing non-Newtonian behavior, such as frame-dragging (Lense-Thirring effect), general relativistic mass shedding, and limiting masses, which will all be investigated in later sections.

#### EINSTEIN'S EQUATION

In order to begin looking at relativistic compact stars we must first establish the basics of relativity. Relativity comes in two forms, special relativity and general relativity. For compact stars, general relativistic effects must be examined due to the stars' enormous densities. The equations used are results of Einstein's field equation, which will be derived below. To obtain Einstein's field equation, several elements are needed. First, since curvature of space-time is the primary factor of general relativity, Ricci curvature is the starting point. The Ricci Tensor is defined as

$$R_{\mu\nu} = \Gamma^{\sigma}_{\mu\sigma,\nu} - \Gamma^{\sigma}_{\mu\nu,\sigma} - \Gamma^{\sigma}_{\kappa\nu}\Gamma^{\kappa}_{\mu\sigma} - \Gamma^{\sigma}_{\kappa\sigma}\Gamma^{\kappa}_{\mu\nu}, \quad (1)$$

where a comma followed by a Greek letter represents a derivative with respect to space-time coordinates, for example  $_{,\sigma} = \partial/\partial x^{\sigma} = \partial_{\sigma}$ . The Christoffel symbol  $\Gamma$  is defined as

$$\Gamma^{\sigma}_{\mu\nu} = \frac{1}{2} g^{\sigma\lambda} (g_{\mu\lambda,\nu} + g_{\nu\lambda,\mu} - g_{\mu\nu,\lambda}). \quad (2)$$

So the Einstein equation can be stated by combining the Ricci Tensor and the energy-momentum tensor,

$$R^{\mu\nu} - \frac{1}{2} g^{\mu\nu} R = 8\pi T^{\mu\nu} \quad (3)$$

where the values of  $c$  and  $G$  have been set equal to 1. It is then often useful to define the Einstein curvature tensor  $G_{\alpha\beta}$  as

$$G^{\mu\nu} \equiv R^{\mu\nu} - \frac{1}{2} g^{\mu\nu} R \quad (4)$$

with the value  $R$  being the Ricci Scalar [8]. Finally, a relation between the Einstein curvature tensor and the energy-momentum tensor can be established, giving rise to Einstein's field equation:

$$G^{\mu\nu} \equiv R^{\mu\nu} - \frac{1}{2} g^{\mu\nu} R = 8\pi T^{\mu\nu}(\epsilon, P(\epsilon)). \quad (5)$$

It is very common to treat neutron star matter as a perfect fluid since many studies propose that they display such characteristics. The energy-momentum tensor of a perfect fluid is

$$T^{\mu\nu} = (dx^\mu/d\tau)(dx^\nu/d\tau)(\epsilon + P) + g^{\mu\nu}P. \quad (6)$$

As usual, pressure  $P$  is a function of energy-density, and  $\tau$  represents the proper time. The energy-momentum tensor, regardless of whether specific for a perfect fluid or not, contains information about the model of the star, namely, the equation of state  $P(\epsilon)$ . It is with this information in combination with Einstein's equations that the properties of compact stars can be determined relativistically.

## SPHERICAL STARS

For stars which are spherically symmetric and non-rotating, the metric is given by

$$ds^2 = -e^{2\Phi(r)}dt^2 + e^{2\Lambda(r)}dr^2 + r^2d\theta^2 + r^2\sin^2\theta d\phi^2 \quad (7)$$

where  $\Lambda(r)$  and  $\Phi(r)$  are metric functions which are radially dependent. It is then straightforward to obtain the covariant components of the metric tensor,

$$g_{tt} = -e^{2\Phi(r)}, g_{rr} = e^{2\Lambda(r)}, g_{\theta\theta} = r^2, g_{\phi\phi} = r^2\sin^2\theta, \quad (8)$$

which then yields after some mathematical manipulation the only non-vanishing Christoffel symbols,

$$\Gamma^r_{tt} = e^{2\Phi(r)-2\Lambda(r)} \Phi'(r), \Gamma^t_{tr} = \Phi'(r), \Gamma^r_{rr} = \Lambda'(r), \Gamma^\theta_{r\theta} = r^{-1}, \Gamma^\varphi_{r\varphi} = r^{-1}, \Gamma^r_{\theta\theta} = -re^{-2\Lambda(r)}, \quad (9)$$

$$\Gamma^\varphi_{\theta\varphi} = \cos\theta/\sin\theta, \Gamma^r_{\varphi\varphi} = -r\sin^2\theta e^{-2\Lambda(r)}, \Gamma^\theta_{\varphi\varphi} = -\sin\theta\cos\theta$$

where primed values indicate a differentiation with respect to the radial coordinate, e.g.  $\Phi' = \partial\Phi/\partial r$ . Upon substituting (6) and (7) into Einstein's field equation (5), one is left with the general relativistic equations of hydrostatic equilibrium for spherically symmetric stars, first proposed by Tolman [9] and Oppenheimer-Volkoff [10],

$$\frac{dP(r)}{dr} = -\left(\frac{\varepsilon(r)m(r)}{r^2}\right)\left(1 + \frac{P(r)}{\varepsilon(r)}\right)\frac{\left(1 + \frac{4\pi r^3 P(r)}{m(r)}\right)}{\left(1 - \frac{2m(r)}{r}\right)} \quad (10)$$

Note that the velocity of light and Gravitational constant use units making  $c = G = 1$ , giving the mass of our sun  $M_{\text{sol}} = 1.475 \text{ km}$ . It is with this equation that properties for spherically symmetric stars were found by means of numerous calculations.

## ROTATING STARS

The equations for compact rotating stars are much more complicated than those of non-rotating stars for several reasons [8]. Since the massive stars are rotating, they flatten at their poles, becoming oblate. This causes the metric for such a system to have a dependence on the polar coordinate  $\theta$ . Also, the star does not depend solely on hydrostatic equilibrium to keep from pulling apart anymore. Gravity will be counteracted by the centrifugal force now being exerted on the star due to its rotation. Consequently, the star can now be more massive than if it were not rotating. However, this in turn means that space-time's geometry around the star is also affected. For a rotating star, the covariant components of the metric tensor are expressed by [8,11]

$$g_{tt} = -e^{2\nu} + e^{2\psi}\omega^2, \quad g_{t\phi} = -e^{2\psi}\omega, \quad g_{rr} = e^{2\lambda}, \quad g_{\theta\theta} = e^{2\mu}, \quad g_{\phi\phi} = e^{2\psi} \quad (11)$$

which therefore leads to the line element

$$ds^2 = g_{\mu\nu}dx^\mu dx^\nu = -e^{2\nu}dt^2 + e^{2\psi}(d\phi - \omega dt)^2 + e^{2\mu}d\theta^2 + e^{2\lambda}dr^2. \quad (12)$$

The change in the line element comes directly from the oblateness of the star caused by rotation, making the metric two-dimensional. In this line element, the angular velocities  $\omega$  of the local inertial frames and the functions  $\mu, \nu, \lambda, \psi$  all depend on the polar angle  $\theta$  and the radial component  $r$ , (there is also the implicit dependence on the star's angular velocity,  $\Omega$ ).

Another interesting point to mention here is the effect of frame-dragging (Lense-Thirring effect). Since space-time around the star is being deformed due to its rotation, the local inertial frames around the star are not at rest with respect to distant stars and get dragged along with the rotating “perfect fluid” inside of the star. The frame-dragging frequency,  $w$ , is defined as

$$w(r, \theta, \Omega) = \Omega - \omega(r, \theta, \Omega). \quad (13)$$

This frequency is important when dealing with rotating stars because it is often necessary to consider the rotation of the interior fluid of the star. As stated earlier, the centrifugal force of the rotating star plays a very important role, and its magnitude is regulated by the rotation rate of the interior fluid with respect to the local inertial frames (inside and out) [12].

However, since we are working with general relativity, these local inertial frames are not at rest with respect to an observer at infinity. They are in fact dragged by the fluid which is rotating inside of the star.

We are also interested in the moment of inertia for compact stars. Only uniformly rotating stars are considered in this paper which are symmetric about their axis of rotation.

To begin, we will start with the expression



$$I^{(\mathcal{A}, \Omega)} \equiv \frac{1}{\Omega} \int_{\mathcal{A}} dr d\theta d\phi T_{\phi}{}^t(r, \theta, \phi, \Omega) \sqrt{-g(r, \theta, \phi, \Omega)} \quad (14)$$

where  $\mathcal{A}$  signifies an axially symmetric region within the star where matter is rotating with the angular velocity  $\Omega$ . The relevant portion of the energy-momentum tensor is given by

$$T_{\phi}{}^t = (\epsilon + P) u_{\phi} u^t \quad (15)$$

With some manipulation and derivation, we are left with the moment of inertia for a compact rotating star,

$$I(\Omega) = 2\pi \int_0^{\pi} d\theta \int_0^{R(\theta)} dr e^{\lambda+\mu+\nu+\Psi} \frac{\epsilon + P(\epsilon)}{e^{2\nu-2\Psi} - (\omega - \Omega)^2} \frac{\Omega - \omega}{\Omega} \quad (16)$$

The relativistic change from the Newtonian expression for the moment of inertia ( $I=2MR^2/5$ ) comes from the curvature of space-time and the effect of local frames being dragged.

## CHAPTER 3

### EQUATION OF STATE

The most important piece of information necessary when calculating properties of compact stars is their equation of state. The equation of state relates the star's energy-density,  $\epsilon$ , to the star's pressure,  $P(\epsilon)$ , a function of the energy-density. For theoretical models of compact stars, different aspects are taken into consideration when the equation of state is created which will be discussed below. For example, the equation of state  $ehv$  (see Table 2) contains nucleons, hyperons, and leptons, but  $ehvpn$  only contains nucleons. Strange quark stars, on the other hand, are actually much simpler in general to design equations of state for. However, many models show quark stars having a nuclear crust, and this crust must be taken into account when calculating properties for these stars.

### CONVENTIONAL NEUTRON-STAR MATTER

For conventional “neutron” stars that contain only nuclear matter, there are 12 equations of state discussed in this paper. Neutron stars begin as the remnants of supernovas, and over time this collection of debris collapses under the force of gravity to a condensed form. These stars are more massive than our sun, but less than 2-3 times  $M_{\text{sol}}$  (typically 1.4  $M_{\text{sol}}$ ). They also only have a radius of approximately 10 km (our sun's radius is approximately 700,000 km), although their density is 10-20 times nuclear density. At the center of the star, the mass-density is on the order of  $2.5 \times 10^{14} \text{ g/cm}^3$  (this value is greater when considering exotic particles) [13,14,8] and its temperature is roughly  $10^{11} \text{ K}$  ( $\sim 100 \text{ MeV}$ ) [27]. Also, the baryon number is approximately  $10^{57}$ ! To put this in perspective, one liter of matter from the core of a neutron star would weigh approximately  $2.45 \times 10^{11}$  tons. As one would conclude from the classical misnomer “neutron” star, the number of neutrons

is extremely high, but these stars also contain a small number of protons and also leptons (for charge neutrality). From chemical equilibrium, the lepton number is regulated, and allowed electrons are highly relativistic (extremely low mass). Consequently, we have the following interaction occurring,

$$n \rightarrow p + e^{-} + \bar{\nu}, \quad (17)$$

from beta decay, although most of the anti-neutrinos are emitted into space early on, causing the star to cool rapidly.

Nuclear matter density will increase from the surface towards the center of the star until it reaches the “neutron drip” density, which is approximately  $4.3 \times 10^{11} \text{ g/cm}^3$  [4]. At this particular density the neutrons are able to leave their nuclei with ease and move freely about, the importance of which will be related to strange quark matter stars in the next section. Properties up to drip density are relatively well known. Even properties between drip density and saturation density are understood to a very good confidence (saturation density represents the density at which nucleon boundaries touch,  $\sim 1.5 \rho_0$ ), but it is the region from saturation density to the center of the star that is highly uncertain. Therefore, equations of state are designed to explain what kind of particles and interactions may be taking place in this unknown area.

As mentioned earlier, it is easier to consider compact neutron stars as being perfect fluids (see equation 6). The equation of state for compact stars must then obey the boundary conditions  $P(r = 0) = P_c = P(\varepsilon_c)$ , where  $\varepsilon_c$  represents the energy-density at the center of the star’s core, and the pressure is computed out to  $P(r = R) = 0$ , signifying that the outer edge of the star has been reached, with the pressure dropping to zero at that limit. The equations of state for neutron star models used in this paper are displayed in Table 1, indicating which

many-body approximation was used for each model. In this table, RH stands for the Relativistic Hartree model, and MIT represents the MIT bag model [15,16,17] (which takes into account quarks). All equations of state were designed with relativistic field theoretical treatments which take into account quantum effects.

**Table 1. Summary of Neutron Star Matter Equations of State. Additional Properties Displayed in Tables 2 and 3**

EOS Label	Many-body approximation	Reference
e2pi	RH	[29]
e300	RH	[30]
e3pi	RH	[30]
eg300b180	RH + MIT	[8]
ehv	RH	[31]
ehvpn	RH	[31]
eg240m78	RH	[13]
eg240b180	RH + MIT	[13]
ewal-cfl-mixed	RH + MIT	[32]
NJLEOSNM	RH + MIT	[33]
NMtoNQMEOSM	RH + MIT	[33]
NMtoSQMEOSM	RH + MIT	[33]

As mentioned before, the composition of each star in question determines the design of the equation of state. In Table 2, the composition and interaction for each neutron star model used in this paper is shown. It should be mentioned here that NJLEOSNM, NMtoNQMEOSM, and NMtoSQMEOSM are new equations of state from Jefferson Laboratory that correspond to Nambu-Jona-Lasinio (NJL) models which represents a four fermion interaction.

**Table 2. Properties of Equations of State Listed in Table 1**

EOS Label	Composition	Interaction
e2pi	N, H, L + $\pi$	$\sigma$ , $\omega$ , $\rho$ meson exchange is the same for all EOSs
e300	N, H, L	
e3pi	N, H, L + $\pi$	
eg300b180	H, H, L + u, d, s quark matter	
ehv	N, H, L	
ehvpn	N	
eg240m78	N, H, L	
eg240b180	N, H, L + u, d, s quark matter	
ewal-cfl-mixed	N, H, L + u, d, s quark matter	
NJLEOSNM	N, H, L	
NMtoNQMEOSM	N, H, L + u, d, s quark matter	
NMtoSQMEOSM	N, H, L + u, d, s quark matter (2SC)	

In this table (Table 2), N stands for nucleons, H for hyperons, and L for leptons.  $\pi$

represents pion condensate. In Table 3, the discussed equations of state are shown with some of their corresponding properties which have affected their design directly.

**Table 3. Properties of Nuclear Matter at Saturation Density of Equations of State from Table 1. The Quantities in this Table are: Energy per Baryon E/A, Compression Modulus K (Defines Curvature of EOS at  $\rho_0$ ), Effective Nucleon Mass  $M^*$  ( $\equiv m^*_N/m_N$ ), and Symmetry Energy  $a_{\text{sym}}$**

EOS Label	E/A	$\rho_0$	K	$M^*$	$a_{\text{sym}}$
	(MeV)	(fm <sup>-3</sup> )	(MeV)	(MeV)	(MeV)
e2pi	-15.95	0.145	200	0.8	36.8
e300	-16.3	0.153	300	0.78	32.5
e3pi	-16.3	0.153	200	0.8	36.8
eg300b180	-16.3	0.153	300	0.70	32.5
ehv	-15.98	0.145	285	0.77	36.8
ehvpn	-15.98	0.145	285	0.77	36.8
eg240m78	-16.3	0.153	240	0.78	32.5
eg240b180	-16.3	0.153	240	0.78	32.5
ewal-cfl-mixed	-16.0	0.160	245	0.74	34.0
NJLEOSNM	-15.0	0.160	250	0.75	32.0
NMtoNQMEOSM	-15.0	0.160	250	0.75	32.0
NMtoSQMEOSM	-15.0	0.160	250	0.75	32.0

The equation of state ewal-cfl-mixed represents a model that is composed of color superconducting quark matter. Quarks are described by three colors: red, green, and blue, and come in six flavors: up, down, strange, charmed, top and bottom [18,19,20,21]. The colors represent the charges that are associated with the strong nuclear force, and each flavor has a different mass and charge (two charge possibilities). Since the stars are so dense, the interaction between quarks and gluons is weak, and therefore the quarks experience asymptotic freedom. Even though the quarks are charged ( $+2/3$  or  $-1/3$ ), bulk quark matter must be color neutral and charge neutral. Furthermore, up and down quarks have mass of just a few MeV, and strange quarks typically have mass around 150-300 MeV. Recently it was shown (28) that cold quark matter forms a color superconductor, which will be either in the color-flavor locked (CFL) phase where we assume that strange quark mass  $\approx$  u,d quark mass  $\approx 0$ , or in the two-flavor (2SC) superconducting phase where strange quark mass is large enough to not be considered, allowing up and down quarks to pair. The ewal-cfl-mixed model has a superfluid gap of  $\sim 100$  MeV, however there is only a gap on the magnitude of KeV to a few MeV for the 2SC phase. Eg240b180 and eg300b180 also account for up, down, and strange quarks.

## **STRANGE MATTER**

Another theorized class of compact stars is strange quark matter stars. Such stars would consist of absolutely stable deconfined up, down, and strange quarks, and possibly other exotic particles. These stars could be bare, and also may have a nuclear (hadronic) crust. The properties of these crusted stars in particular are very fascinating to astrophysicists.

Strange quarks are believed by many to be the absolute ground state of the strong nuclear force, i.e. the building blocks of nuclear matter [1,2]. It is known that nucleons are composed of up and down quarks (with protons having two up quarks and one down quark, and neutrons having one up quark and two down quarks), but hyperons contain strange quarks, and the energy/baryon value is claimed to be less than 930 MeV (E/A of stable nuclear matter), making hyperons more stable. This will be shown for the strange quark EOS. A simple model for strange matter is the MIT bag model [15,16,17], which can be thought of as a spherical “bag” full of free quarks. For strange quark matter stars, the equation of state is actually very simple,

$$P = (\varepsilon - 4B)/3 \quad (18)$$

where P represents pressure,  $\varepsilon$  represents energy-density, and B is the bag constant which is a function of density. For strange quark matter,  $B^{1/4}$  varies from 145 MeV to 160 MeV [7]. Using the equation  $E/A = 4\pi^2 B/\mu^3$ , it is straightforward to show that for bag constant  $B^{1/4} = 145$  MeV, the corresponding E/A value is 829 MeV, and for  $B^{1/4} = 160$ ,  $E/A = 915$  MeV. Both of these values are indeed smaller than stable nuclear matter, and therefore,  $145 \text{ MeV} \leq B^{1/4} \leq 160 \text{ MeV}$  represents the viable range for absolutely stable strange quark matter.

Strange quark mass is greater than the both up and down quark masses, and consequently from chemical equilibrium and charge neutrality (necessary precision  $\sim 10^{-37}$  net charge/baryon) [4], the strange core for the 2SC phase contains a determinable number of highly relativistic electrons. From these electrons, the core creates an electric dipole layer on its surface with field strength  $\sim 10^{17}$ - $10^{19}$  V/cm. If we consider a strange star that has a nuclear crust enveloping its rotating core, this electric dipole layer is strong enough to displace the charge of the crust layer and suspend the crust above the core, even allowing the

core and crust to rotate at different frequencies (differential rotation). As mentioned in the last section, the maximum crust density is limited by the neutron drip density ( $4.3 \times 10^{11} \text{ g/cm}^3$ ), since all free neutrons will be transformed to strange quark matter upon contact. This neutron drip density is less than the least massive neutron star by several orders of magnitude [27], so we can conclude that the minimum strange star mass with a crust of density<sub>max</sub> = density<sub>drip</sub> is less than a neutron star of minimum mass. It is straightforward to show that if we keep the inner crust density maximized at the “drip density”, then as the mass of strange core increases, the thickness of the crust decreases, and vice versa.



## CHAPTER 4

### RESULTS

This study of compact stars is based on a broad collection of equations of state. One aim is to offer a correction to the many-body technique used to solve the nuclear many-body problem ( $10^{57}$  interacting particles) by replacing the static quantum potential with another that accounts for meson exchange in order to explain exotic phenomena for these stars. When examining the properties of relativistic compact stars, it is often easiest to display the properties in graphical form. The usual properties of interest are: mass, radius,  $\Omega_{\text{kepler}}$ , moment of inertia, etc. As will be seen in the next section, these properties offer an immense amount of information in relatively straightforward plots.

One particular interest examined in this paper is the surface gravity of compact stars. This has been looked at for both neutron and strange stars. The surface gravity ( $g_s$ ) for relativistic compact stars is an important constraint when considering different models since a higher value would indicate more exotic phases due to higher densities. This value is also important for stellar cooling and the infall velocity for accretion in binary systems. The surface gravity for typical neutron stars is approximately  $10^8$  times stronger than that of the sun due to its extremely dense nature, and is even greater for strange stars. Since  $g_s$  is calculated, it is determined by the equation of state because the properties of the stars are also dependent on the EOS. To calculate  $g_s$ , we use the equation

$$g_s = GM/[R^2(1 - 2GM/Rc^2)^{1/2}] \quad (19)$$

where  $G$  is the gravitational constant,  $M$  is the star's mass,  $R$  the star's radius, and  $c$  is the speed of light. Because the values of  $g_s$  are very high (typically  $\sim 10^{14}$  g/cm<sup>2</sup>), it is more

convenient to use the notation  $g_{s,14} = g_s/10^{14}$ . After being aware of this notation, a simpler equation for calculating  $g_s$  is

$$g_{s,14} = (15.21 \text{ g/cm}^2)(x^2/(1-x)^{1/2})(M/M_{\text{sol}}) \quad (20)$$

where we have designated  $x = 2GM/Rc^2$ . Surface gravity will be examined further in this section.

## NEUTRON STARS

As mentioned throughout the paper, the mass and radii of stars are very important properties. Astronomers and astrophysicists use both properties not only alone, but also in determining other properties of the stars. Shown in Figure 1 is a mass versus radius plot of all nuclear matter models used in this paper (rotating and non-rotating). This plot is very common when studying compact stars, and it is obvious that as the radius increases, the mass decreases (after the limiting mass), as mentioned earlier. The knowledge of limiting masses is of key importance to determine the number of black holes in any given galaxy. Stars to the left of the mass peak of each stellar sequence are unstable against radial oscillations and will collapse to black holes. The Schwarzschild limit indicates the definitive point of no return to black holes for compact stars. Mass-radius plots for strange quark stars are quite different, which will be discussed in the next section. Note that the mass for the models from Jefferson Lab drop off much more quickly. Also, it is evident that the rotating models are more massive than their non-rotating counterparts. As mentioned earlier, this is caused by the centrifugal force from rotation which pulls on the star and allows it to hold more mass as it counteracts the force of gravity. A recently measured neutron star mass in a radio pulsar was  $(1.35 \pm 0.04) M_{\text{sol}}$  [25], which agrees with Figure 1. Similarly, the candidates for heavy neutron stars in Table 4 also agree.

**Table 4. Candidates for Heavy Neutron Stars**

Star Candidate	Mass (units of $M_{\text{sol}}$ )	Reference
Cyg X-2	1.78 +/- 0.23	[35]
Vela X-1	1.88 +/- 0.13	[36]
J0751 + 1807	2.1 +/- 0.4/-0.5	[37]
4U 1820 – 30	2.2 – 2.3 +/- 0.1	[38]

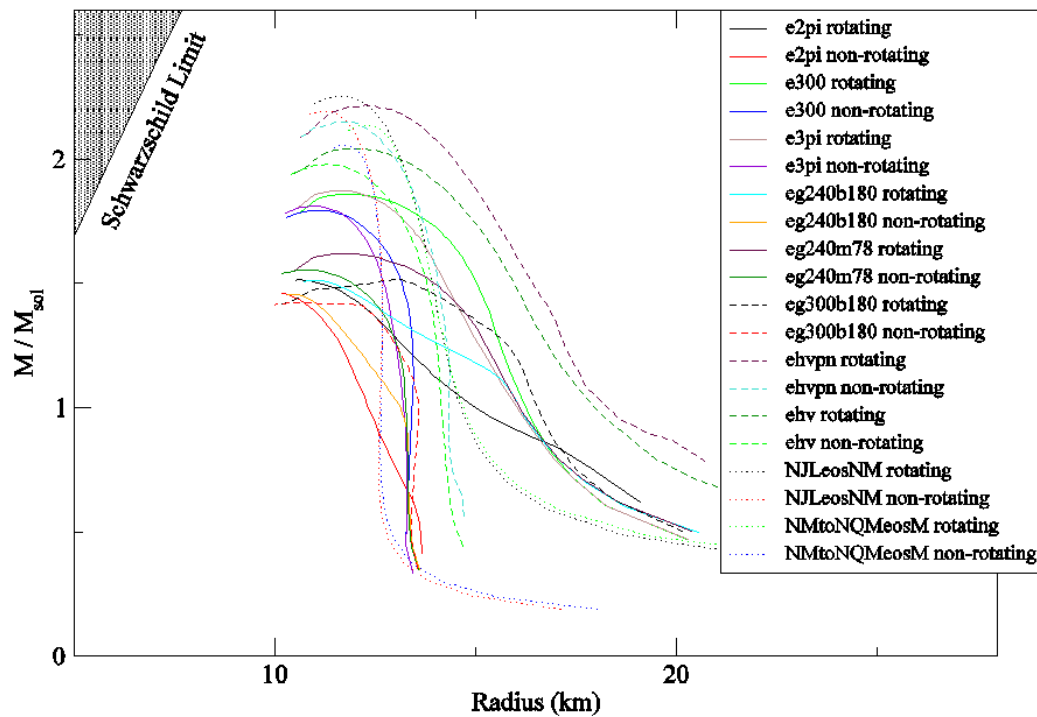


**Figure 1. Comparison of mass (in solar masses) versus radius (km) for this series of compact stars. This figure compares these properties for both rotating and spherically symmetric versions of these stars.**

In section 3 it was stated that the equation of state describes all aspects of the model for each star, so that all properties can be determined by it. Each EOS contains pressure values as a function of energy-density. This is shown in Figure 2 for the whole sequence of models used, including those from the Jefferson Laboratory. In Figure 2, the line  $P = \epsilon$

represents the limiting EOS, where pressure is equal to the corresponding energy-density. If an EOS were designed that crossed this boundary, it would not be physically acceptable since it would violate the condition of causality, i.e. pressure must increase monotonically. In essence,

$$v_s/c = (\partial P/\partial \epsilon)^{1/2} \quad (21)$$

with  $v_s$  representing the sound velocity, and  $c$  the speed of light. If  $\partial P/\partial \epsilon > 1$ , then  $v_s$  would be greater than  $c$ , which is not possible. Also, a curve representing a pure neutron gas is shown indicating the lower limit for stars. Note that NJLeosNM is the stiffest model since it does not account for any quark matter in the star. As the number of degrees of freedom increase in an EOS, the softer the EOS becomes. NJLeosNM also has a greater pressure than the other models, although the values of mass and radius are very near each other, as can be seen in Figure 1 (note: the abrupt change in pressure for the NMtoSQMeosM curve may represent a phase transition. This has been investigated more thoroughly in a recent Jefferson Lab paper. Such a phase transition may imply that there is no mixed phase of deconfined quark matter and hadrons within the star). It should also be noted that the EOSs from Jefferson Lab have pressures  $P(\epsilon)$  that extend to much higher values, but typically neutron stars do not have pressure greater than  $2000 \text{ MeV}/\text{fm}^3$ , so those additional points have been discarded prior to calculations.

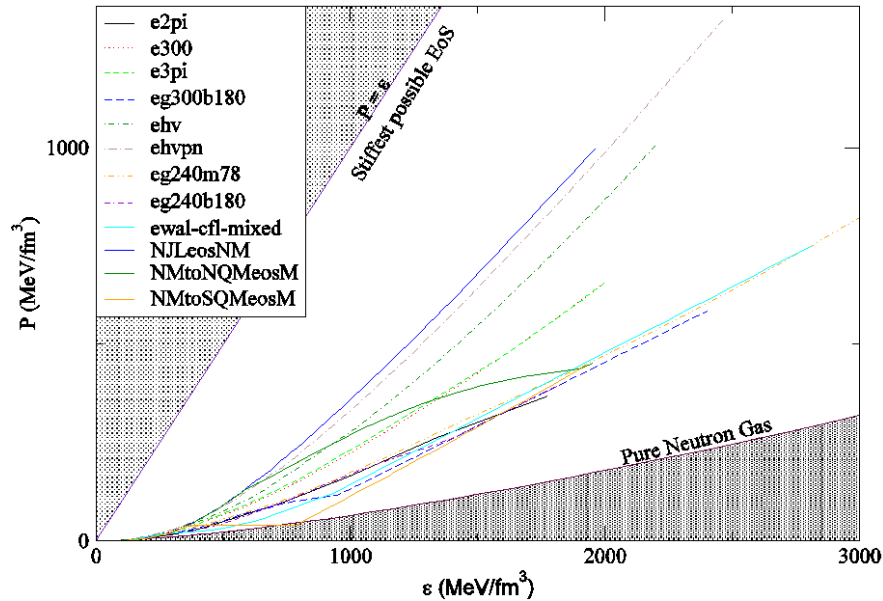


**Figure 2. Comparison of pressure versus energy-density for compact star equations of state. The uppermost line represents the limit EOS, where pressure equals energy-density. Any EOS past it would violate causality.**

Another question that astrophysicists have is, how dense can “neutron” stars actually be? Density can be indicative of pressure, particle number, and a variety of other properties, so such a relation is of great interest. Also, if the maximum “neutron” star density can be determined, then scientists will be able to truly establish which compact stellar objects are “neutron” stars, and which may even need their own new class. The mass-density (central density) plots for non-rotating (Figure 3) and rotating (Figure 4) stars are very interesting as they show the range of densities for different masses. As expected, the rotating series can sustain greater masses, and the curves are also shifted slightly to the left from loss of pressure arising in rotating. This range of possible densities can be more easily seen in Figures 5, 6, and 7. The more massive the star is, the less likely the existence of exotic matter (lower density), however, some of these models can sustain great masses as well extremely high

densities which may indicate heavy “neutron” stars with possible mixed cores, another subject of very great significance.

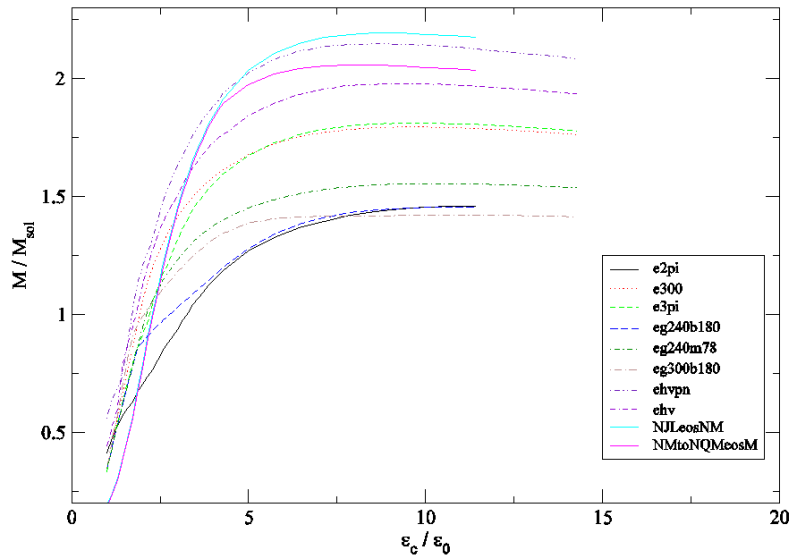


Figure 3. Mass versus energy-density for sequence of non-rotating neutron stars.

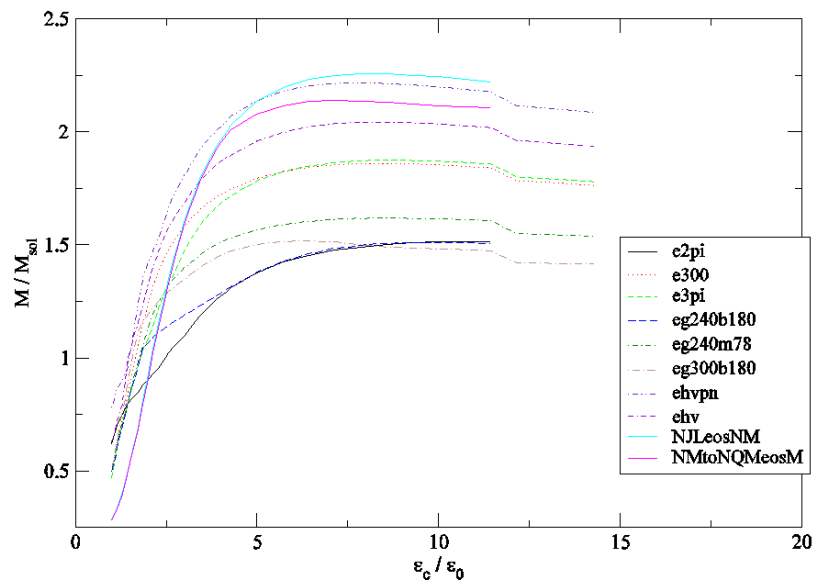
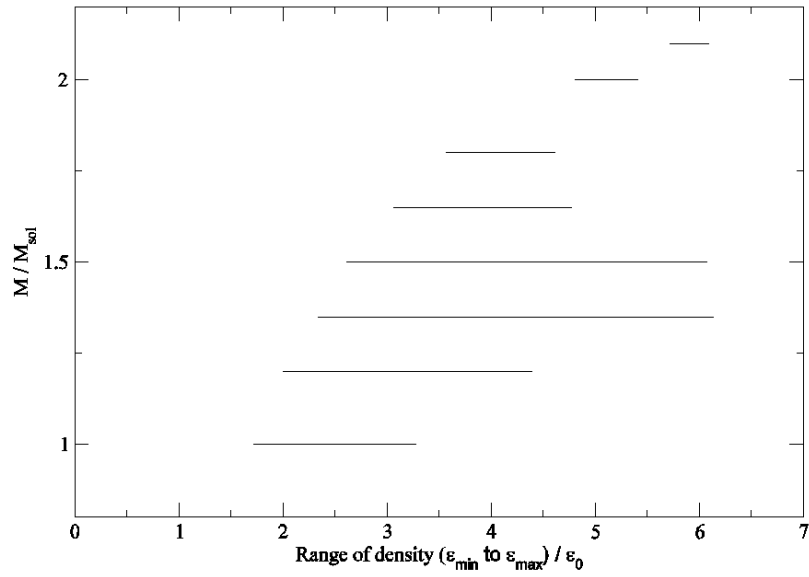
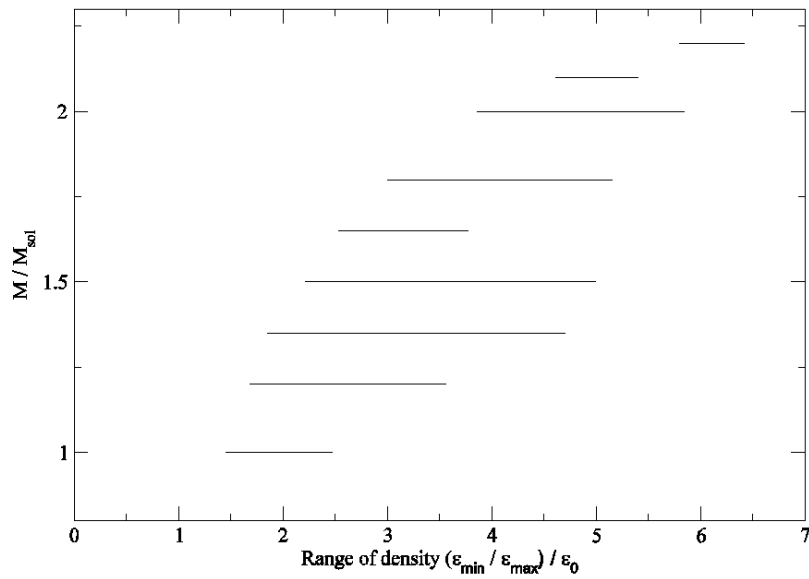


Figure 4. Mass versus energy-density for sequence of rotating neutron stars.



**Figure 5.** Mass versus the range of possible densities for the sequence of non-rotating neutron stars.



**Figure 6.** Mass versus the range of possible densities for the sequence of rotating neutron stars.

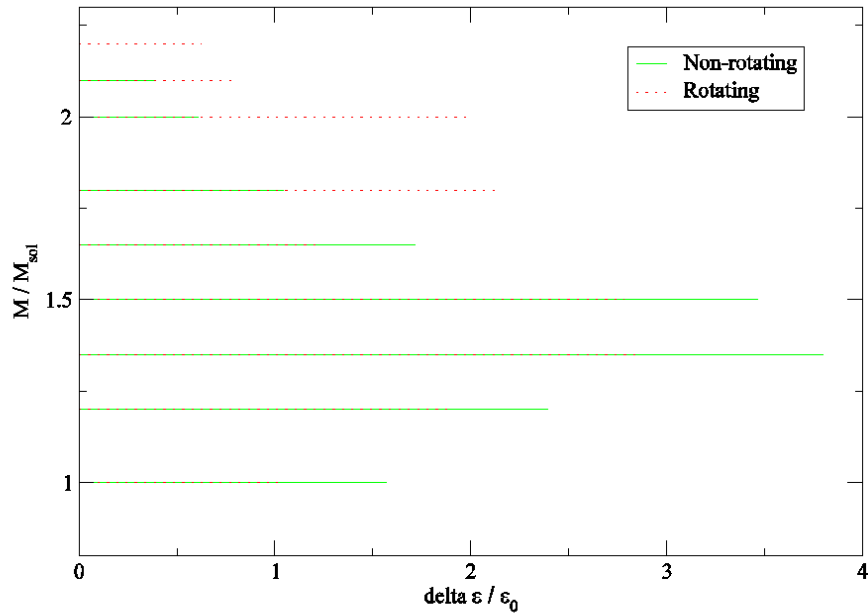


**Figure 7. Comparison of mass versus range of possible densities for this sequence of rotating and non-rotating stars.**

Recall that the moment of inertia for a rotationally deformed star is given by

$$I(\Omega) = 2\pi \int_0^\pi d\theta \int_0^{R(\theta)} dr e^{\lambda+\mu+\nu+\psi} \frac{\varepsilon + P(\varepsilon)}{e^{2\nu-2\psi} - (\omega - \Omega)^2} \frac{\Omega - \omega}{\Omega} \quad (16)$$

since it is treated within the framework of Einstein's equations. This is caused by the deviation in the star's frequency and the frequency of local inertial frames about the star  $\{1 > (\Omega - \omega)/\Omega\}$ . As a result, there is a drastic change in moment of inertia when compared to the classical treatment. The moment of inertia increases with the mass of the stars (Figure 8) until the limiting mass is reached, as it does in the classical case, however, the rate of increase is much more prominent.



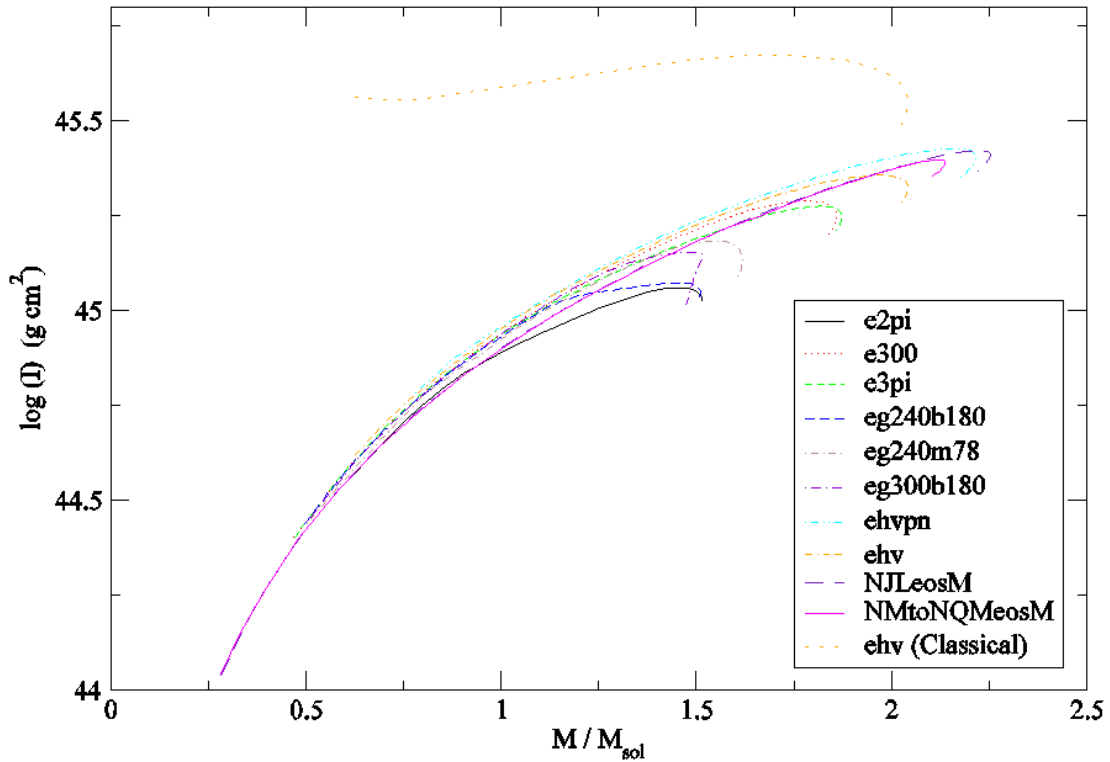


**Figure 8. Moment of Inertia for compact stars versus their mass (in solar masses). The classical moment of inertia for EOS *ehv* has also been shown for comparison. Note the substantial change when relativistic effects are taken into account.**

The surface gravity for these stars was first plotted with the corresponding masses (Figure 9), but a mass of  $1.3 M_{\text{sol}}$  was selected to compare them on the same scale. The points shown are not precisely  $1.3 M_{\text{sol}}$ , but were chosen for being the closest to that value in the calculated data. Calculations were later redone to produce Figure 10 which shows surface gravity for exact masses of 1.3, 1.35, and  $1.4 M_{\text{sol}}$ . There is a striking difference between ewal-cfl-mixed and the other EOSs. As stated earlier, this equation of state represents a model that is color superconducting quark matter, and is approximately 25 times as dense as atomic nuclei. The values of  $g_{s,14}$  for masses 1.35 and  $1.4 M_{\text{sol}}$  were actually too

great to incorporate on this plot. There are some neutron star models which have even greater values for  $g_{s,14}$  (as large as  $g_{s,14} \sim 6 \text{ cm/s}^2$ ) [26], but are not examined in this paper.

Calculations were also made to determine these stars' limiting masses, the greatest mass that they can have without becoming unstable and falling apart. Figure 11 shows the limiting masses versus their corresponding surface gravities ( $g_{s,14}$ ). Although ewal-cfl-mixed has a large value for its surface gravity, it also has the smallest limiting mass. This is from the quark matter contained in this model and its extremely high density. Figure 12 then shows the full range for these models. Surface gravity for strange quark matter stars will be discussed in the next section.

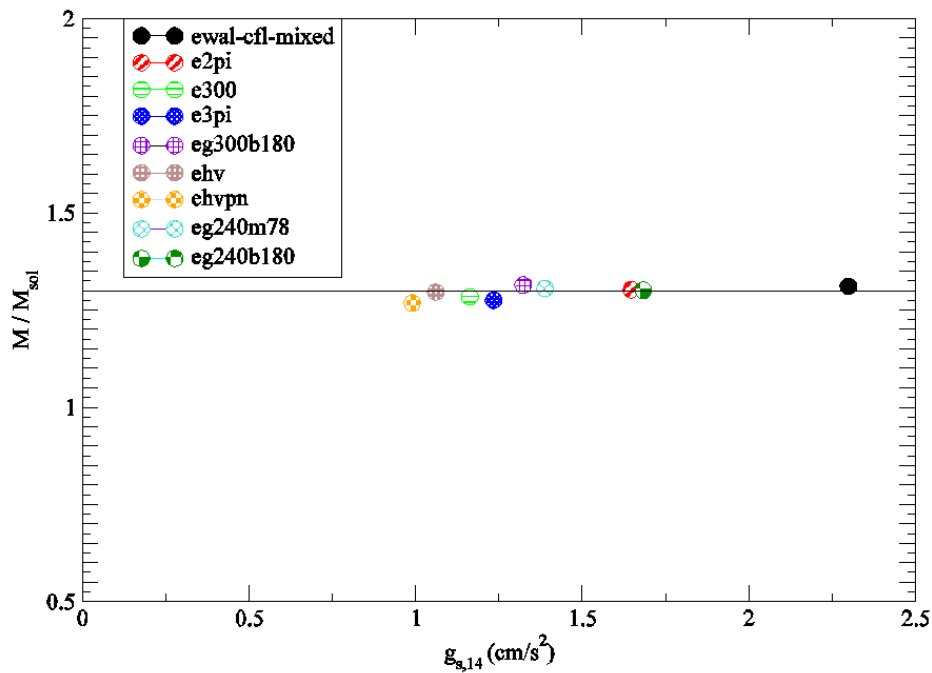


**Figure 9. Mass (in solar masses) versus surface gravity in units of  $10^{14} \text{ cm/s}^2$  for star masses near 1.3 solar masses.**

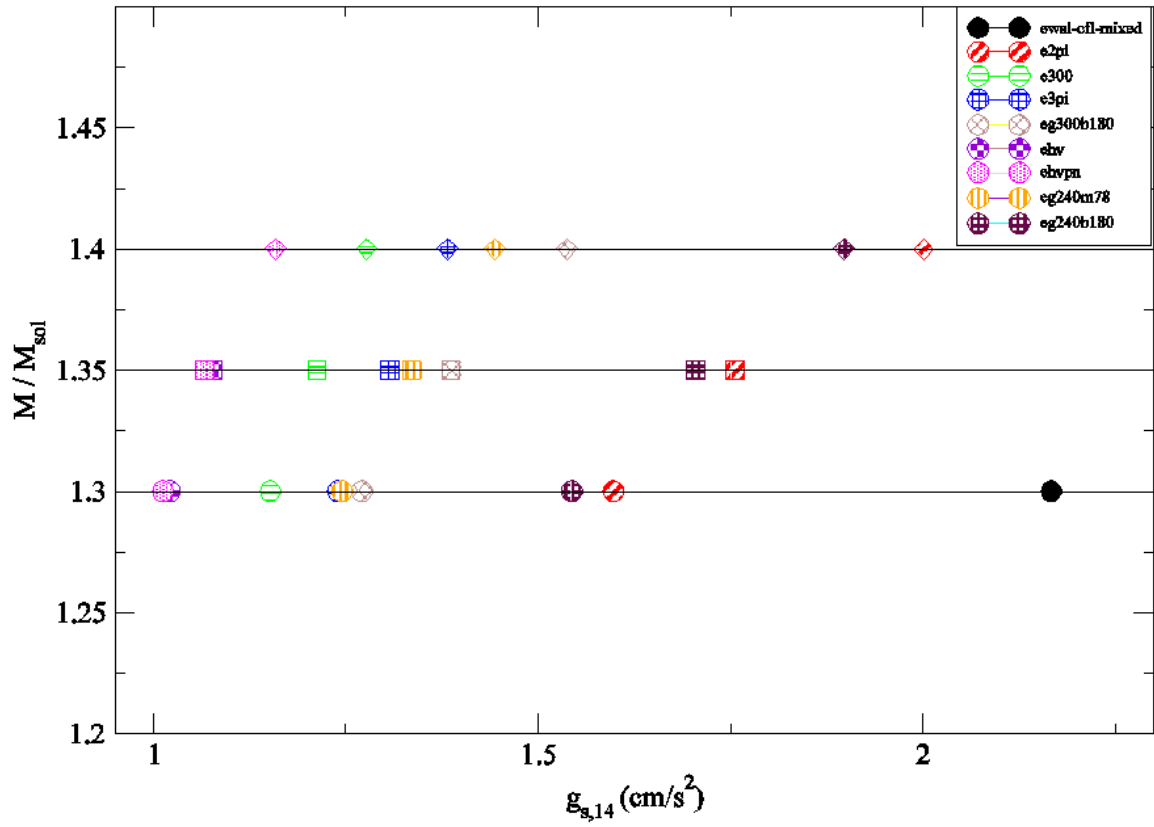


Figure 10. Mass (in solar masses) versus surface gravity in units of  $10^{14} \text{ cm/s}^2$  for exact masses of 1.3, 1.35, and 1.4 Msol. Ewal-cfl-mixed points for 1.35 and 1.4 Msol have values greater than allowed on this plot.

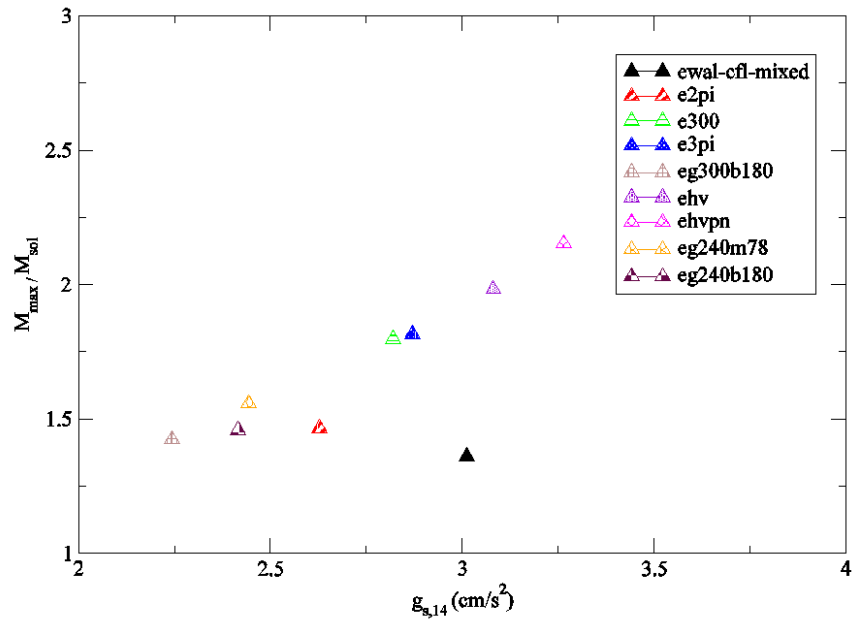


Figure 11. Shown here are the limiting masses and corresponding surface gravities (in units of  $10^{14} \text{ g/cm}^2$ ) for this sequence of compact stars.

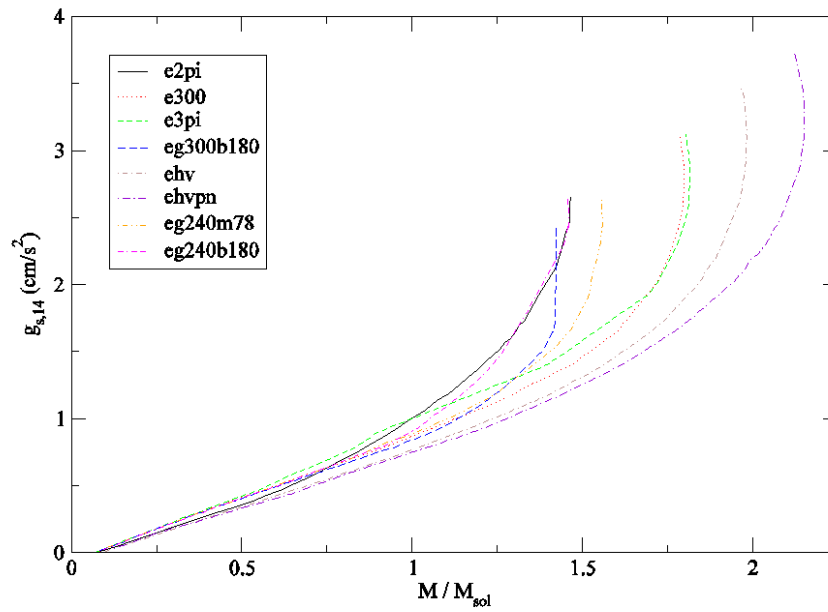


Figure 12. Surface gravity versus mass for neutron stars. Full range is shown.

It is known that compact stars can spin very rapidly, even up to 716 Hz (J1748-2446ad,  $R < 16$  km), which makes them extremely relativistic (716 Hz for a star with radius 16 km yields a rotational surface velocity of  $7.71980 \times 10^7$  m/s,  $\sim 0.26c$ ). However, there is an absolute limit to how large the rotational frequency of the star can be, and that is referred to as the Kepler frequency ( $\Omega_{\text{kepler}}$ ) (also known as the mass-shedding frequency/mass-shedding angular velocity). A star exceeding its Kepler frequency would eject matter into space. This is simple to show classically. Since we are trying to find the maximal angular frequency, we equate the gravitational force to the centrifugal force,

$$m\Omega^2 R = mM/R^2 \quad (22)$$

solving for  $\Omega$ , we are left with

$$\Omega = (M/R^3)^{1/2} \quad (23)$$

This is the classical value of the Kepler frequency for a rotating object, but since we are dealing with such massive stars, relativistic effects must be taken into account. The rough approximation

$$\Omega_K \approx 0.65(M/R^3)^{1/2} \quad (24)$$

can be used since it is very accurate, however, this does not give the exact value because it cannot be calculated from a direct formula. It can only be generated as a self-consistency condition [13] from Einstein's equations for relativistic rotating stars.

Recall from equation 12, the line element for stars is equal to  $ds^2 = g_{\mu\nu}dx^\mu dx^\nu = -e^{2\nu}dt^2 + e^{2\psi}(d\phi - \omega dt)^2 + e^{2\mu}d\theta^2 + e^{2\lambda}dr^2$ . To calculate the Kepler frequency, we consider only a solitary point on the star's surface. Therefore,  $r = \theta = \text{constant}$ , so we can say that the line element is now equal to

$$ds^2 = (e^{2\nu} - e^{2\psi}(\Omega - \omega)^2)dt^2 \quad (25)$$

After several calculations and manipulations, we arrive with a Kepler frequency of

$$\Omega_K = \omega + (\omega'^2/2\psi) + e^{v-\psi}(v'/\psi + (\omega' e^{v-\psi}/2\psi)^2)^{1/2} \quad (26)$$

We are interested in the Kepler period of the stars, which is simply

$$P_K = 2\pi/\Omega_K. \quad (27)$$

The calculated values of Kepler periods ( $P_K$ ) for these EOSs have been displayed in Figure 14 showing  $P_K$  versus  $M/M_{\text{sol}}$ . Alternatively, the frequency  $\nu$ , has been plotted against the mass in Figure 13.

Again, since NJLEOSNM is the stiffest EOS, it can support the largest mass. As can easily be seen, these equations of state can account for the observed stars.

However, if gravity wave instabilities were taken into consideration, the values shown would decrease by 30-40%, but these curves represent the absolute limit for rotation.

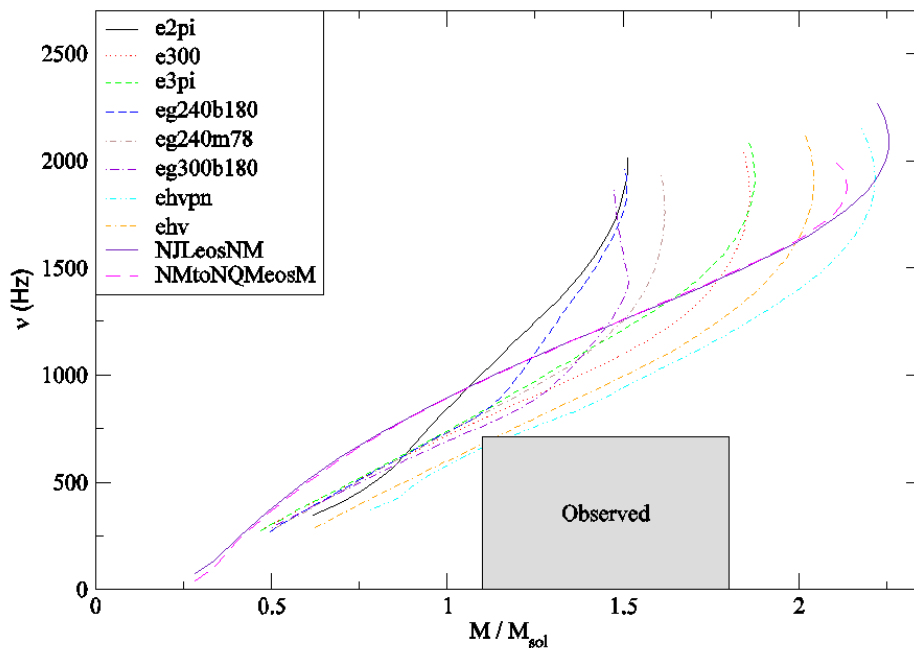


**Figure 13. Kepler (mass shedding) frequency of compact stars versus their masses (in units of solar mass). Frequencies of observed stars have been shaded. Observed stars rotate below the mass shedding frequency.**

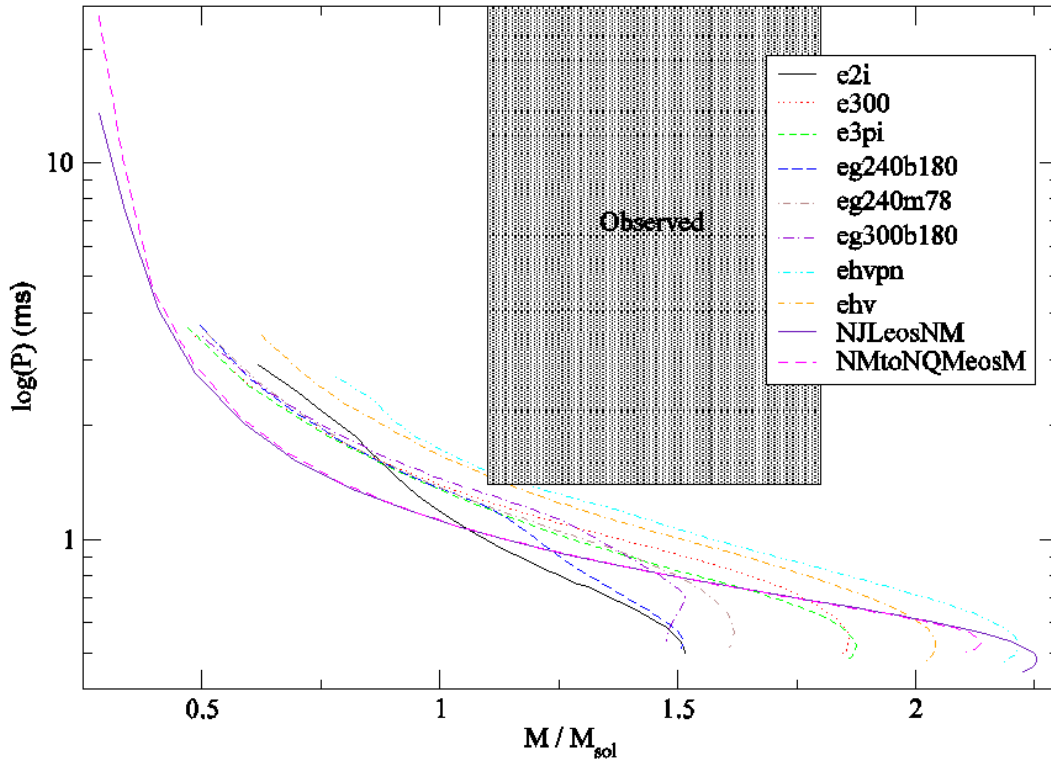


**Figure 14. Kepler (mass shedding) period versus mass (in solar masses) for sequence of stars. Observed stars rotate above the mass shedding period.**

### QUARK STARS

As previously stated, the strange quark star model used for this paper utilizes the MIT bag model equation of state  $P = (\epsilon - 4B)/3$ . Just as within the last section, the first plot shown for strange quark stars is a mass versus radius comparison. On the contrary, it is strikingly different than Figure 1. Shown in Figure 15 are three curves, all calculated with bag constant = 145 MeV. The solid line represents the core of the strange star. To produce the other two curves, the crust density for the model was fixed at  $4 \times 10^8 \text{ g/cm}^3$  and  $4 \times 10^{11} \text{ g/cm}^3$  and then calculations were run. This plot allows the reader to determine the mass of

the crust (for a given crust density) and radius on the curve. Note that an increase of only a few orders of magnitude makes a substantial increase in the mass of the crust (the electric dipole gap is negligible in this plot since its size is on the magnitude of only a few fm). Figure 16 shows the same plot as Figure 15, except that for this graph calculations were made using the bag constant = 160 MeV. It is also obvious that as the bag constant is increased, the limiting mass decreases.

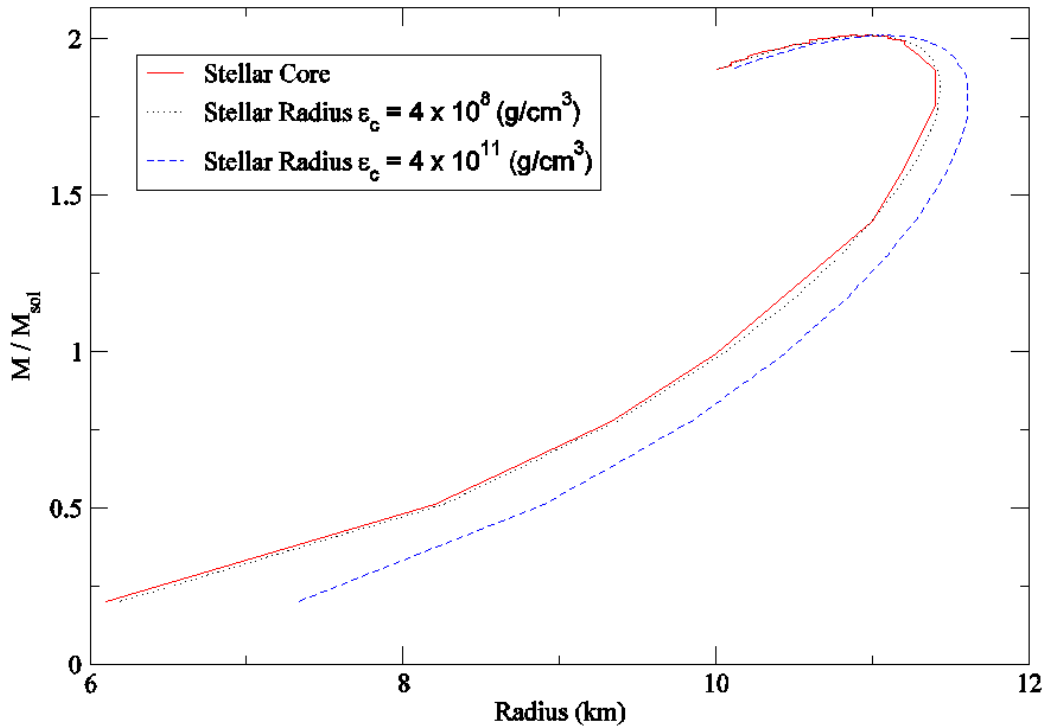


**Figure 15. Comparison of mass versus radius for a strange quark star with bag constant  $B^{1/4} = 145$  MeV. The crust energy-density has been set for two different values.**



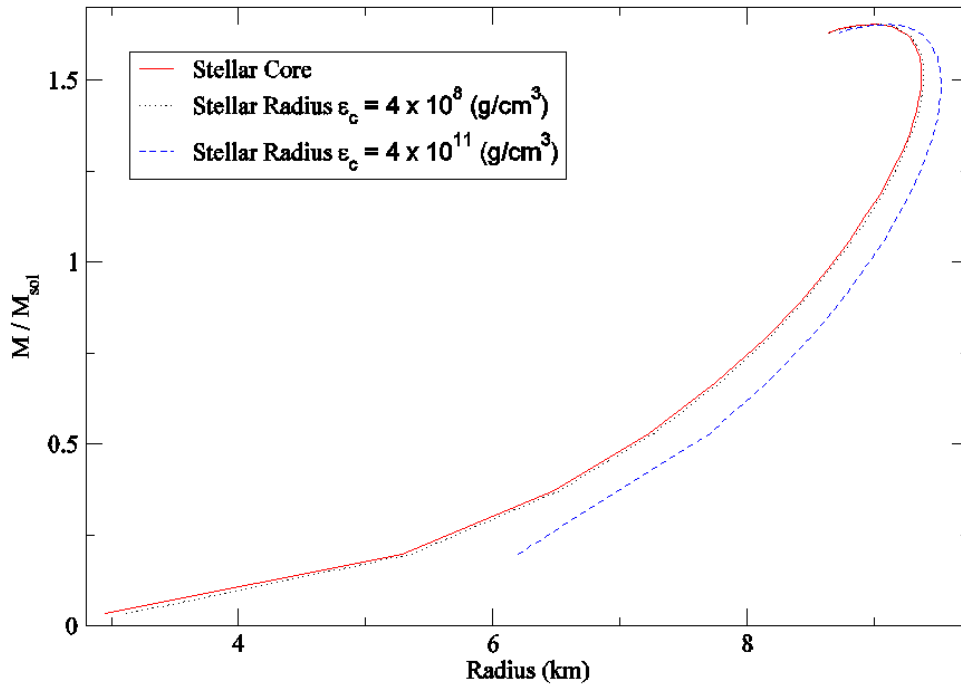


**Figure 16. Comparison of mass versus radius for a strange quark star with bag constant  $B/4 = 160$  MeV. The crust energy-density has been set for two different values.**

Another plot of mass versus radius is displayed in Figure 17, but here the energy-density of the crust has not been predetermined and fixed for calculations. Different bag constants have again been presented, and also models for rotating and non-rotating stars. The rotating models for these stars can support greater masses because of the centrifugal force, as discussed in section 3. If mass were calculated conventionally by  $M = 4\pi \int_0^R r^2 \varepsilon(r) dr = \frac{4\pi R^3}{3}$ , then the mass would increase to infinity since  $M \propto R^3$ , however this clearly does not happen, and there *is* a limiting mass which is a direct result of Einstein's equations.

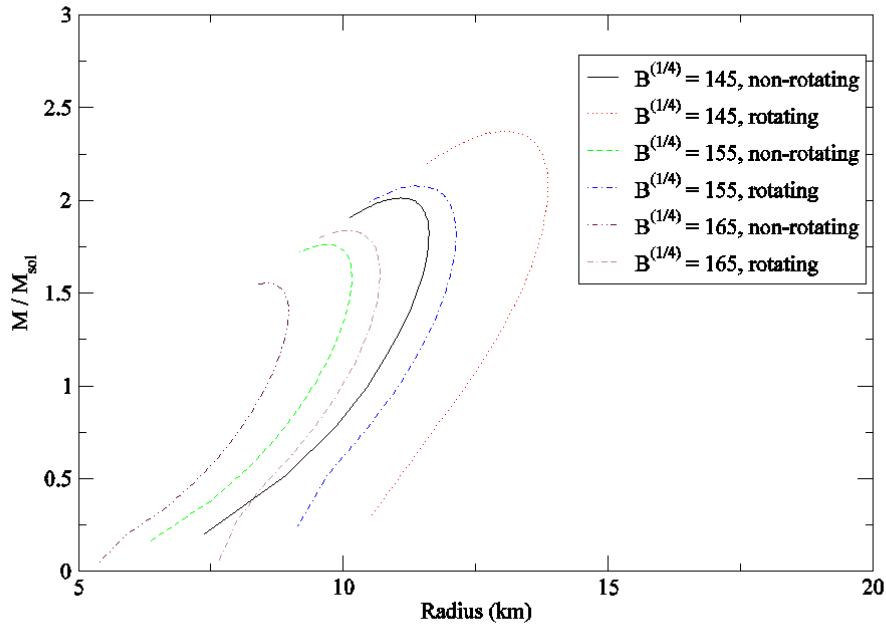


**Figure 17. Mass (in solar masses) versus radius for strange quark stars. Shown are a comparison of rotating and non-rotating sequences for different bag constants.**

The surface gravity for two models of strange quark stars is shown in Figure 18, with bag constants  $B^{1/4} = 145$  MeV and 160 MeV. As  $g_{s,14}$  is a function of mass, it should and does peak at the limiting mass of the strange stars.

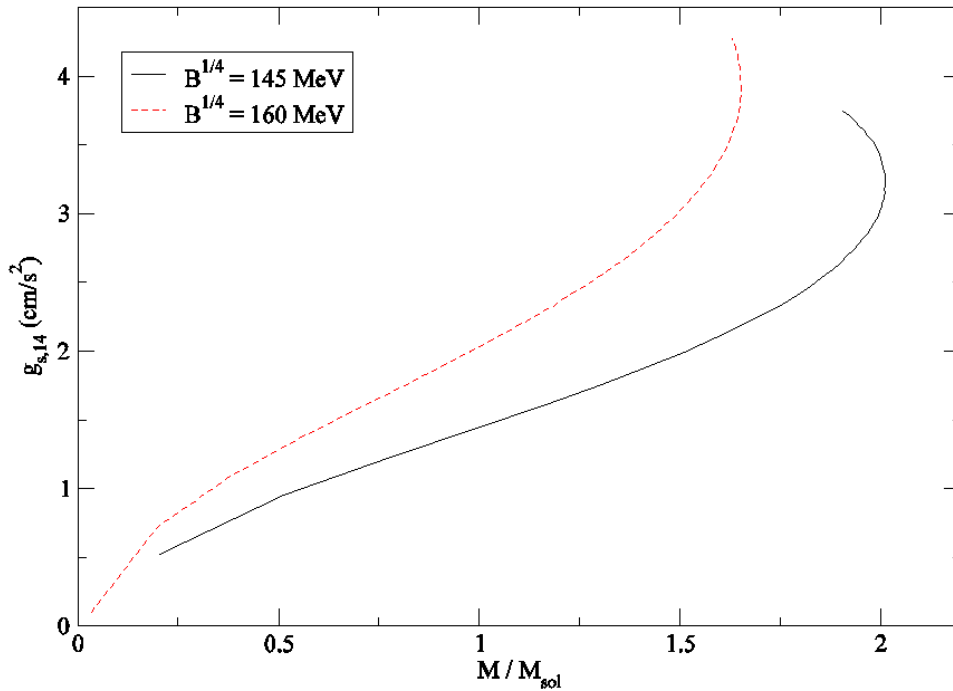


**Figure 18. Surface gravity as a function of mass (in solar masses) for strange quark stars with different bag constants.**

When we analyze these equations of state, we are looking for particular properties of strange stars ( $M$ ,  $R$ ,  $g_{14}$ ,  $A$ , etc.) in order to determine if these objects are associated with a number of astrophysical phenomena, such as:

- Pulsar Glitches
- X-ray bursts
- Interpretation of millisecond pulsars (MSP)
- Gamma-ray burst models

A very important property that is investigated in these phenomena is the baryon number of such stars. The baryon number of the crust for strange stars versus the number for the core

(Figure 19) is nearly linear. However, at a certain core number (corresponding to the limiting mass), the crust baryon number does “turn” and begin to decrease, as well as the core number.

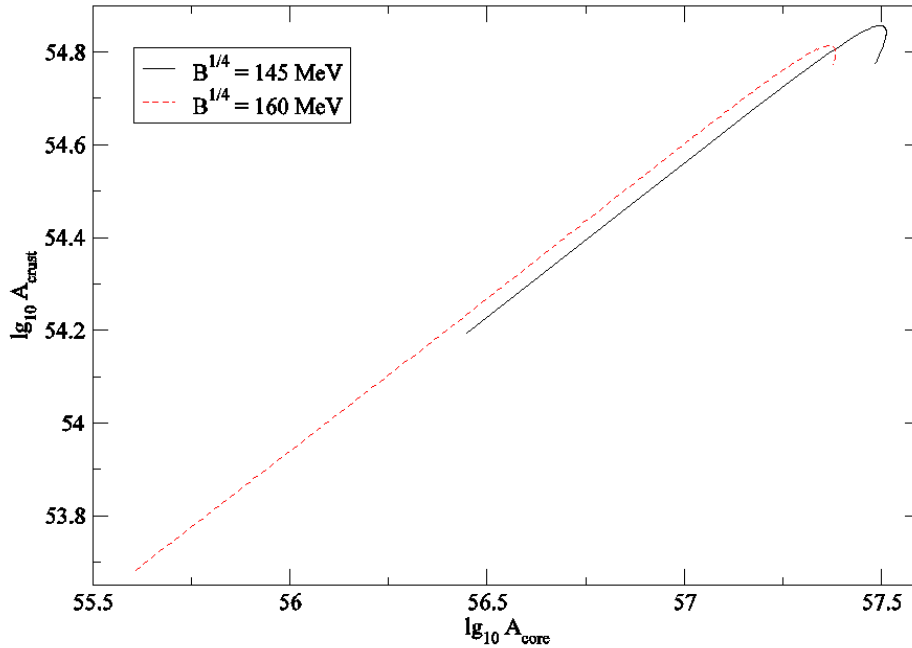


**Figure 19. Baryon number of crust versus baryon number of core for bag constants  $B^{1/4} = 145 \text{ MeV}$ ,  $160 \text{ MeV}$ .**

The mass and thickness of the crust are dependent upon the core’s composition and properties. Crust mass is an important factor in various stellar behaviors, such as pulsar glitches and cooling behavior. Although these phenomena are not discussed in the paper, they are very complicated problems that are currently being investigated in other projects. Crust mass and baryon number will be examined further by myself in future work to be done on a new EOS [34] which takes into consideration changing quark masses in matter. This new EOS is an improved model to the standard model used in this paper as the MIT bag model assumes that quark masses stay constant. Figures 20, 21, and 22 show these properties

for the standard bag model which was used in this paper ( $m_{u,d,s} = \text{constant}$ ), and will be compared to properties of the new EOS mentioned.

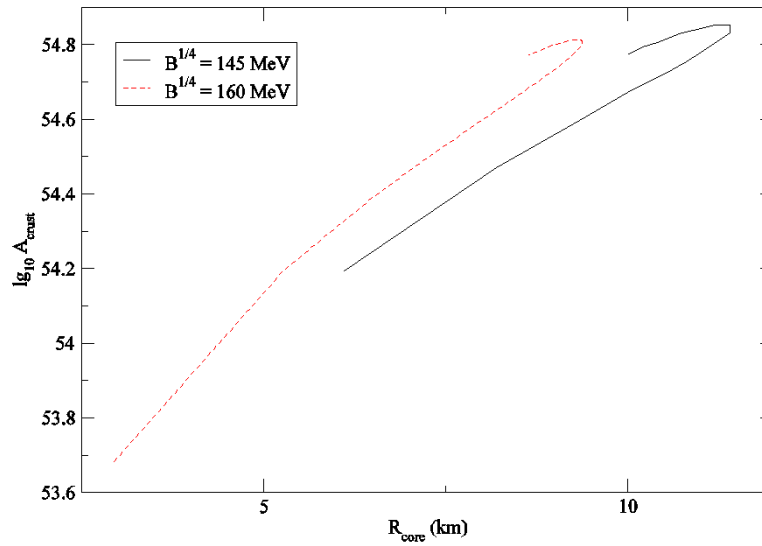


**Figure 20.** Baryon number of crust versus radius of strange quark matter core for bag constants  $B^{1/4} = 145 \text{ MeV}$ ,  $160 \text{ MeV}$ .

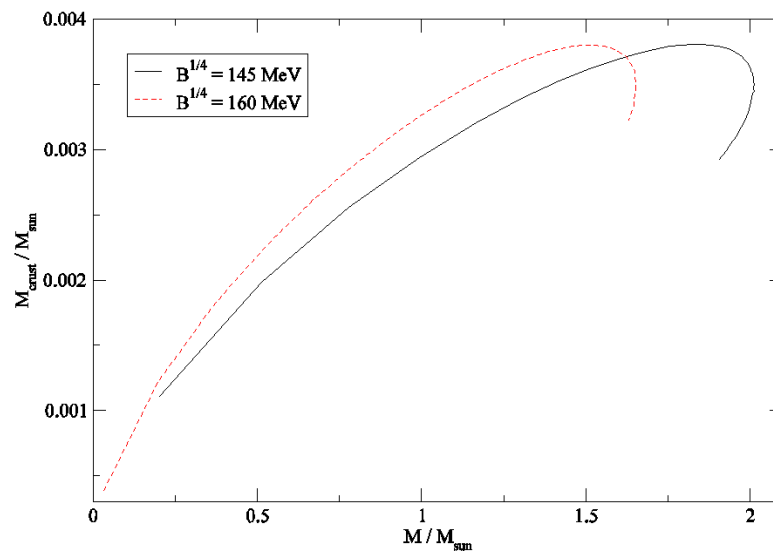


**Figure 21.** Crust mass versus total mass of strange quark star for bag constants  $B^{1/4} = 145 \text{ MeV}$ ,  $160 \text{ MeV}$ .

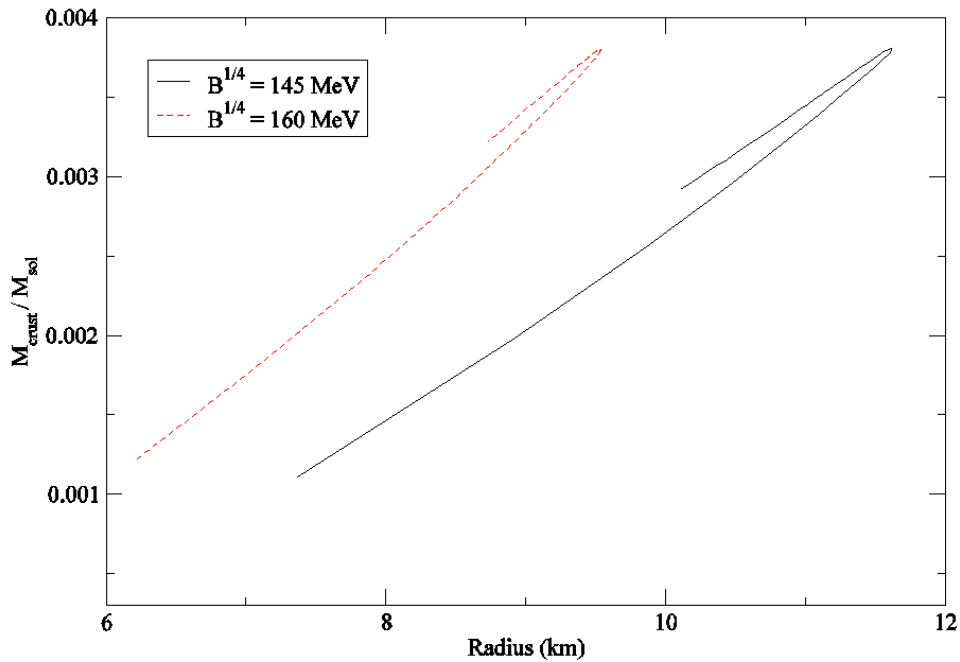


**Figure 22. Crust mass versus total radius of strange quark star for bag constants  $B^{1/4} = 145 \text{ MeV}$ ,  $160 \text{ MeV}$ .**

## CHAPTER 5

### SUMMARY

The nature of “neutron” stars causes them to have enormous pressures in their cores, allowing extraordinary and exciting properties, one of which is the possibility of breaking down neutrons and protons to their elementary particles, quarks. Their super-dense characteristic also allows them to host other exotic particles (hyperons, quarks, boson condensates) and presents them as an ideal laboratory for interesting phenomena and interactions. Since the density of these stars is so great, a relativistic treatment must be used when performing calculations; however, this does allow and explain fascinating properties

such as frame-dragging, existence of limiting masses, and general-relativistic mass shedding. It should also be noted that certain relations can be understood and predicted by these relativistic calculations, ranging from mass-radius curves to surface gravity and spin frequencies.

Because strange quark matter is of such great interest in the astrophysics and nuclear physics communities, the idea that this matter may be at the cores of these stars, or that stars may actually be completely composed of strange quark matter is quite fascinating, especially since quark deconfinement may happen at densities as low as  $2.5\rho_0$ , a value easily obtainable in these EOSs. If these stars do contain quark matter it will be color superconducting, and nuclear crust (if any) will be suspended above the core over a superconducting gap [4]. Furthermore, if rotating, the cores may even rotate at different frequencies (differential rotation) than the crust enveloping them. The properties of strange quark stars are strikingly different than those of conventional neutron stars.

Finally, a key feature is that many properties of a neutron star are determined by the nuclear equation of state. For the equations of state used to model the neutron stars in this paper, careful consideration was made in their design depending on the particular cores desired to explain. However, for quark stars following the MIT bag model, the EOS is straightforward, with a linear curve of pressure versus energy-density. It is important to note here that not all strange star equations of state follow such a design. For example, an EOS from reference [34] (Figure 23) has been used to plot pressure versus energy-density, and is also compared to the MIT bag model for bag constants = 145 MeV and 160 MeV. This plot is not linear, and is actually more closely approximated by a parabolic curve. It is important

to investigate such stars since they may represent a substantial portion of dark matter, and strange nuggets could even convert all nuclear matter it contacts into strange quark matter.

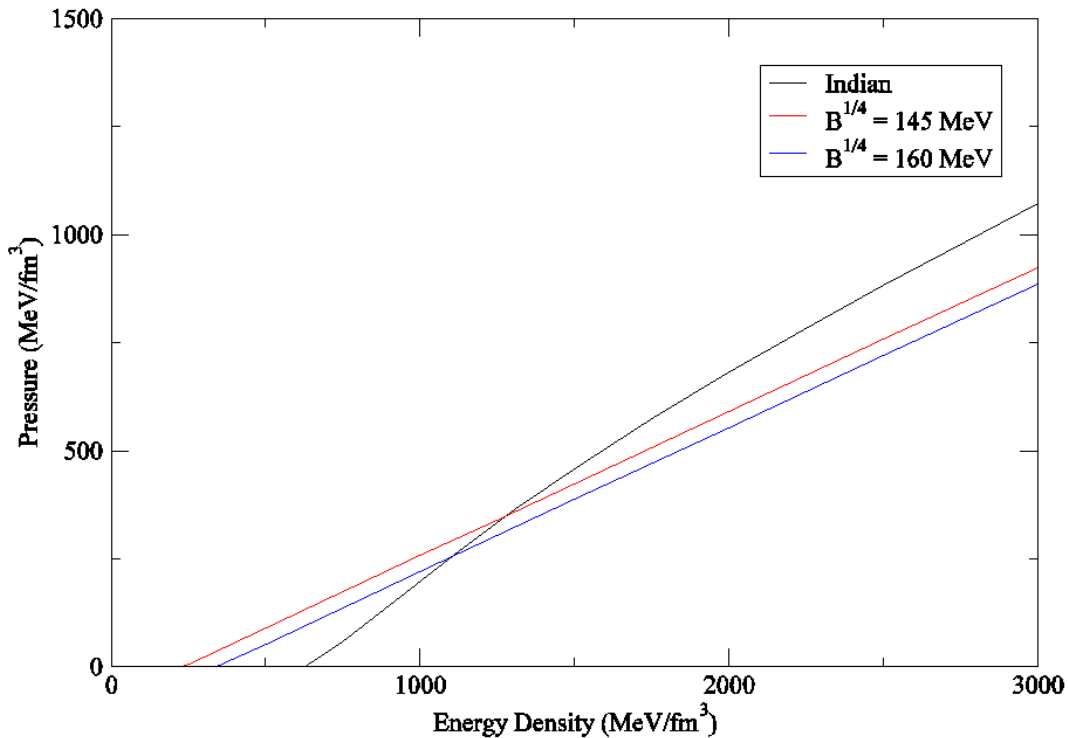


**Figure 23.** Comparison of equations of state for the *Indian model* to the MIT bag model,  $B^{1/4} = 145$  MeV and 160 MeV.

The aim of this work is to aid in alleviating some of the huge uncertainties associated with compact star equations of state. These uncertainties arise from several aspects, such as: the many-body approximations (Hartree, Hartree-Fock, Brueckner-Hartree-Fock), relativistic effects (Schrödinger versus field theoretical approach), the “building blocks” of neutron star matter (phase transitions, quarks, boson condensates), and the true ground state of the strong interaction. This paper offers several important conclusions with respect to these compact stars. In particular:



- 1) Maximal density of “neutron” stars
- 2) Possibility of actually containing exotic phases/particles inside the core (boson condensates, quark matter, or solely nucleons)
- 3) For heavy “neutron” stars, the equation of state must become stiffer due to fewer degrees of freedom, and central-density decreases.

Also, three new EOSs from Jefferson Lab (NJL model) and the rapidly rotating 716 Hz star were compared to many accepted EOSs of state for neutron stars. Although the rapidly rotating star *can* be explained by these equations of state, no solid conclusions can be made yet on the NJL models. Further study is required, and is currently being done. These findings will help in determining whether or not observed “neutron” stars are actually what we believe to be neutron stars at all, and if classified as so, will give astronomers and astrophysicists a collection of properties on which to begin new research.

The future of “neutron” star and strange star research has enormous potential, not only for studies specific to the stars themselves, but also to many different aspects of astrophysics. Some possibilities include:

- Further study of strange stars for the M. Dey, J. Dey, M. Bagchi EOS [34]
- Differential rotation (rigid-body was studied in this paper)
- “Hot” neutron stars (“cold” stars were studied in this paper,  $T \leq 1$  MeV)
- Density dependent microscopic theories
- Gravity-wave instabilities [27]

These studies will ultimately be able to help us understand the true nature of the matter that fills our universe.

## REFERENCES

- <sup>1</sup> A.R. Bodmer, Phys. Rev. D **4**, 1601 (1971).
- <sup>2</sup> E. Witten, Phys. Rev. D **30**, 272 (1984).
- <sup>3</sup> H. Terazawa, INS-Report-**338**, INS, Univ. of Tokyo, 1979; J. Phys. Soc. Japan, **58**, 3555 (1989); **58**, 4388 (1989); **59**, 1199 (1990).
- <sup>4</sup> N.K. Glendenning, F. Weber, Astrophys. J. **400**, 647, 648 (1992).
- <sup>5</sup> C. Alcock, E. Farhi, and A. V. Olinto, Astrophys. J. **310**, 261 (1986).
- <sup>6</sup> C. Alcock and A. V. Olinto, Ann. Rev. Nucl. Part. Sci. **38**, 161 (1988).
- <sup>7</sup> J. Madsen, Lecture Notes in Physics **516**, 162 (1999).
- <sup>8</sup> F. Weber, *Pulsars as Astrophysical Laboratories for Nuclear and Particle Physics*, High Energy Physics, Cosmology and Gravitation Series (IOP Publishing, Bristol, Great Britain, 1999).
- <sup>9</sup> R. C. Tolman, Phys. Rev. **55**, 364 (1939).
- <sup>10</sup> J. R. Oppenheimer and G. M. Volkoff, Phys. Rev. **55**, 374 (1939).
- <sup>11</sup> J. L. Friedman, J. R. Ipser, and L. Parker, Astrophys. J. **304**, 115 (1986).
- <sup>12</sup> J. B. Hartle, Astrophys. J. **150**, 1005 (1967).
- <sup>13</sup> N.K. Glendenning, *Compact Stars, Nuclear Physics, Particle Physics, and General Relativity*, 2nd ed. (Springer-Verlag, New York, 2000)
- <sup>14</sup> J. M. Lattimer and M. Prakash, Astrophys. J. **550**, 131 (2001).
- <sup>15</sup> A. Chodos, R.L. Jaffe, K. Johnson, C.B. Thorne, V.F. Weisskopf, Phys. Rev. D **9**, 3471 (1974).
- <sup>16</sup> A. Chodos, R.L. Jaffe, K. Johnson, C.B. Thorne, Phys. Rev. D **10**, 2599 (1974).
- <sup>17</sup> E. Farhi, R.L. Jaffe, Phys. Rev. D **30**, 2379 (1984).
- <sup>18</sup> K. Rajagopal, F. Wilczek, in: M. Shifman (Ed.), *The Condensed Matter Physics of QCD, At the Frontier of Particle Physics/Handbook of QCD*, World Scientific, 2001.
- <sup>19</sup> M. Alford, Ann. Rev. Nucl. Part. Sci. **51**, 131 (2001).
- <sup>20</sup> M. Alford, K. Rajagopal, F. Wilczek, Phys. Lett. B **422**, 247 (1998).
- <sup>21</sup> R. Rapp, T Schaefer, E.V. Shuryak, M. Velkovsky, Phys. Rev. Lett. **81**, 53 (1998); Ann. Physics **280**, 35 (2000).
- <sup>22</sup> N.K. Glendenning, Mod. Phys. Lett. A **5**, 2197 (1990).
- <sup>23</sup> J. Madsen and M.J. Olesen, Phys. Rev. D **43**, 1069 (1991).
- <sup>24</sup> R.R. Caldwell and J.L. Friedman, Phys. Lett. B **264**, 143 (1991).

- <sup>25</sup> D. Chakrabarty and S.E. Thorsett, *Astrophys. J.* **512**, 288 (1999).
- <sup>26</sup> M. Bejger and P. Haensel, *Astron. & Astrophys.* **420**, 988 (2004).
- <sup>27</sup> F. Weber, *Prog. In Part. And Nuc. Phys.* **54**, 193-288 (2005).
- <sup>28</sup> F. Weber, A.T. Cuadrat, A. Ho, P. Rosenfield, *Strangeness in Compact Stars*, (astro-ph/0602047)
- <sup>29</sup> N. K. Glendenning, *Phys. Rev. Lett.* **57**, 1120 (1986)
- <sup>30</sup> N. K. Glendenning, *Nucl. Phys. A* **493**, 521 (1989)
- <sup>31</sup> F. Weber and M. K. Weigel, *Nucl. Phys. A* **505**, 779 (1989)
- <sup>32</sup> M. Alford and S. Reddy, *Phys. Rev. D* **67**, 074024 (2003)
- <sup>33</sup> P. Wang, S. Lawley, D.B. Leinweber, A.W. Thomas, A.G. Williams, *Phys. Rev. C* **72**, 045801 (2005); S. Lawley, W. Bentz, A.W. Thomas, *Phys. Lett. B* **632**, 495 (2006)
- <sup>34</sup> M. Dey, I. Bombaci, J. Dey, S. Ray, B.C. Samanta, *Phys. Lett. B* **438**, 123 (1998); M. Bagchi, S. Ray, M. Dey, J. Dey, *Strange Star Equation of State with a Modified Richardson Potential*, (astro-ph/0509703)
- <sup>35</sup> J.A. Orosz, E. Kuulkers, *Mon. Not. R. Astron. Soc.* **305**, 132 (1999)
- <sup>36</sup> H. Quaintrell, A.J. Norton, T.D.C. Ash, P. Roche, B. Willems, T.R. Bedding, I.K. Baldry, R.P. Fender, *A&A* **401**, 313-323 (2003)
- <sup>37</sup> D.J. Nice, E.M. Splaver, I.H. Stairs, O. Loehmer, A. Jessner, M. Kramer, J.M. Corder, *A 2.1 Solar Mass Pulsar Measured by Relativistic Orbital Decay*, (astro-ph/0508050)
- <sup>38</sup> W. Zhang, T.E. Strohmayer, J.H Swank, *Astrophys. J.* **482**, L167 (1997)

**APPENDIX**  
**SAMPLE EOS**

## SAMPLE EOS

Shown here is the input file for the equation of state ewal-cfl-mixed. The first column is the pressure (MeV/fm<sup>3</sup>), the second is the energy-density (MeV/fm<sup>3</sup>), and the third is the baryon number density (1/fm<sup>3</sup>).

Wall\_CFL\_mixed

70

1.41367000E+01	2.93171000E-02	0.0150
5.67855000E+01	2.49804000E-01	0.0600
9.76008000E+01	1.27001000E+00	0.1032
1.39848000E+02	3.53664000E+00	0.1469
1.75728000E+02	6.51535000E+00	0.1833
2.18953000E+02	1.14398000E+01	0.2263
2.59167000E+02	1.73448000E+01	0.2653
3.17679000E+02	2.07321000E+01	0.3210
3.69495000E+02	2.28265000E+01	0.3700
4.13003000E+02	2.51981000E+01	0.4110
4.50195000E+02	2.78010000E+01	0.4458
4.82624000E+02	3.06011000E+01	0.4760
5.37507000E+02	3.66957000E+01	0.5267
5.83732000E+02	4.33413000E+01	0.5689
6.24650000E+02	5.04541000E+01	0.6059
6.62444000E+02	5.79820000E+01	0.6397
6.98678000E+02	6.58959000E+01	0.6717
7.34229000E+02	7.41799000E+01	0.7028
7.87769000E+02	8.72860000E+01	0.7490
8.24673000E+02	9.64794000E+01	0.7805
8.64062000E+02	1.06052000E+02	0.8137
9.10006000E+02	1.16040000E+02	0.8520
9.34081000E+02	1.21217000E+02	0.8720
9.81873000E+02	1.37258000E+02	0.9111
1.01488000E+03	1.48347000E+02	0.9379
1.06621000E+03	1.65591000E+02	0.9790
1.10168000E+03	1.77502000E+02	1.0070
1.13817000E+03	1.89753000E+02	1.0356
1.17571000E+03	2.02351000E+02	1.0647
1.21430000E+03	2.15301000E+02	1.0944
1.25397000E+03	2.28610000E+02	1.1247
1.29475000E+03	2.42286000E+02	1.1554
1.33664000E+03	2.56334000E+02	1.1868
1.37968000E+03	2.70762000E+02	1.2187
1.42388000E+03	2.85576000E+02	1.2512
1.46926000E+03	3.00784000E+02	1.2843
1.49240000E+03	3.08537000E+02	1.3010
1.53959000E+03	3.24348000E+02	1.3349
1.58801000E+03	3.40569000E+02	1.3695
1.61269000E+03	3.48836000E+02	1.3870
1.66301000E+03	3.65687000E+02	1.4224
1.71462000E+03	3.82966000E+02	1.4584

1.74091000E+03	3.91769000E+02	1.4767
1.76753000E+03	4.00682000E+02	1.4951
1.82178000E+03	4.18840000E+02	1.5323
1.87738000E+03	4.37449000E+02	1.5702
1.90570000E+03	4.46925000E+02	1.5893
1.93436000E+03	4.56517000E+02	1.6087
1.99273000E+03	4.76050000E+02	1.6478
2.02245000E+03	4.85993000E+02	1.6676
2.05253000E+03	4.96056000E+02	1.6875
2.08297000E+03	5.06239000E+02	1.7076
2.11377000E+03	5.16542000E+02	1.7279
2.14494000E+03	5.26969000E+02	1.7483
2.20839000E+03	5.48191000E+02	1.7897
2.24068000E+03	5.58989000E+02	1.8106
2.27335000E+03	5.69913000E+02	1.8317
2.30639000E+03	5.80965000E+02	1.8529
2.37364000E+03	6.03452000E+02	1.8959
2.40785000E+03	6.14890000E+02	1.9177
2.44245000E+03	6.26459000E+02	1.9396
2.47745000E+03	6.38160000E+02	1.9616
2.51285000E+03	6.49994000E+02	1.9839
2.54865000E+03	6.61962000E+02	2.0063
2.58486000E+03	6.74064000E+02	2.0289
2.62147000E+03	6.86303000E+02	2.0516
2.69594000E+03	7.11193000E+02	2.0976
2.73379000E+03	7.23846000E+02	2.1209
2.77207000E+03	7.36639000E+02	2.1443
2.81077000E+03	7.49573000E+02	2.1680

END OF DATA

## ABSTRACT OF THE THESIS

Properties of Relativistic, Compact Stars

by

Alexander W Ho

Master of Science in Physics

San Diego State University, 2006

Compact stars are extremely dense objects with very interesting properties. Not only are they of great interest to astrophysicists, but their dense nature provides an excellent testing area for a variety of phenomena and exotic particles that may prove significant to many different areas of physics as well. One particular subject is that of strangeness and strange quark stars. This paper investigates such stars as well as their nuclear counterparts, neutron stars. The properties of relativistic neutron stars are examined as well as the impact of strangeness on compact astronomical objects.